International Journal of Applied Mathematics

Volume 38 No. 3s, 2025

ISSN: 1311-1728 (printed version); ISSN: 1314-8060 (on-line version)

INTEGRATED MODEL FOR DEEP LEARNING AND MACHINE LEARNING FOR THE IDENTIFICATION OF SKIN CANCER

Mrs. Seema Ravindra Baji, Dr. Sahebrao Bhaurao Bagal, Dr.Sachin Vasant Chaudhari[3], Dr. Balasaheb Shrirangrao Agarkar[4]

[1]Research Scholar, Department of E&Tc, Sanjivani College of Engineering, Kopargaon, Maharashtra, Savitribai Phule Pune University, Pune.

bajiseema1@gmail.com

[2]Research Guide, Department of E&Tc, Sanjivani College of Engineering, Kopargaon, Maharashtra, Savitribai Phule Pune University, Pune.

bagalsb@gmail.com

[3]Research Coordinator, Department of E&Tc, Sanjivani College of Engineering, Kopargaon, Maharashtra, Savitribai Phule Pune University, Pune.

chaudharisachinece@sanjivani.org.in

[4]Head of E&Tc Department, Sanjivani College of Engineering, Kopargaon, Maharashtra, Savitribai Phule Pune University, Pune.

hodetccoe@sanjivani.org.in

Abstract

Skin cancer is a serious and potentially life-threatening condition, making early and accurate diagnosis essential for effective treatment. The most common types of skin cancer are basal cell carcinoma (BCC), squamous cell carcinoma (SCC), and melanoma. Dermatologists rely on skin images to identify the type and severity of these cancers. In recent years, researchers have been developing computer-aided diagnosis systems to assist in early detection. This paper explores a hybrid model that combines machine learning and deep learning techniques to enhance the diagnostic accuracy of skin cancer. Specifically, Convolutional Neural Networks (CNNs) are employed to analyze dermatological images, extracting detailed features that indicate various types of skin cancer. Alongside CNNs, the FractalNet model—a specialized deep learning technique—is used for diagnosis. These models are then integrated with the XGBoost algorithm in parallel. The final diagnosis decision is made through majority voting, ensuring a robust system that can identify both simple and complex features. This hybrid approach, leveraging the different strengths of CNN, FractalNet, and XGBoost, results in a more generalized diagnostic system. The HAM10000 dataset, which includes 10,015

Received: July 25, 2025

International Journal of Applied Mathematics

Volume 38 No. 3s, 2025

ISSN: 1311-1728 (printed version); ISSN: 1314-8060 (on-line version)

dermatoscopic images of pigmented skin lesions, is used for model training. Data augmentation is applied to balance the dataset. For performance evaluation, precision, recall, F1-score, accuracy, and specificity are measured, with an achieved accuracy of 98.69%.

Keywords: Convolution Neural Networks (CNN), FractalNet model, XGBoost algorithm, HAM10000 dataset

Introduction:

Cancer

Cancer is a complex group of diseases characterized by the uncontrolled growth and spread of abnormal cells (1), which can invade and damage surrounding tissues, leading to the formation of tumors. There are many different types of cancer as shown in figure 1, each with its own specific characteristics, risk factors, and treatment options (2). Skin cancer, in particular, can be quite serious in its later stages and significantly impacts the skin (3). According to global cancer statistics for 2023, nearly 1,524,700 cases of skin cancer were reported, resulting in approximately 120,000 deaths (4).

Skin Cancer

A skin carcinoma is a prevalent form of cancer originating within the skin's cellular structure and holds the distinction of being the most widespread cancer globally. Distinguished into several types, the primary classifications encompass Squamous cell carcinoma (SCC), melanoma, and basal cell carcinoma (BCC) (5).

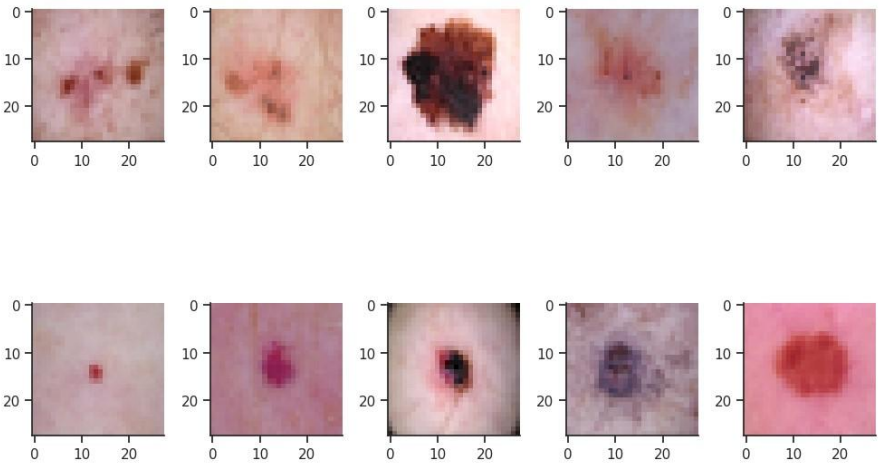

Figure 1: Different skin cancer images

BCC, or basal cell carcinoma is ranked as the most frequent usually the kind of skin cancer manifests on face and neck, which are exposed to the sun, (6). While BCC tends to be locally invasive, its propensity for spreading to other body parts is rare (7). Another type of skin cancer is the SCC (Squamous Cell Carcinoma) stands as second-most prevalent skin cancer, commonly emerging on exposed sun regions for example, the hands, ears, and face (8). Although SCC is less prone to metastasize compared to melanoma, it exhibits a tendency for local aggressiveness. Despite being less common than BCC and SCC, melanoma poses a

Received: July 25, 2025

Volume 38 No. 3s, 2025

ISSN: 1311-1728 (printed version); ISSN: 1314-8060 (on-line version)

higher risk of metastasis to other body parts (9). Melanoma is a pigment-producing cell that originates from melanocytes and can appear anywhere on the body, irrespective of sun exposure. Timely detection is critical, as melanoma's aggressiveness increases with spread.

Risk Factors of skin cancer include extended exposure to ultraviolet (UV) light, whether from the sun or tanning beds, heightens the risk (10). Those with light hair and fair skin, and blue or green the eyes are particularly vulnerable (11). The presence of numerous moles or unusual moles increases the risk, as does skin cancer in the family history (12).

Prevention of these cancer types consist of prominently the sun protection measures, including sunscreen use, protective clothing, and avoidance of excessive sun exposure, particularly during peak hours, are crucial. Regular self-examinations for changes in moles or new growths, coupled with professional skin checks by dermatologists, contribute to preventive efforts. Steering clear of tanning beds is essential to mitigate the risk of skin cancer.

Detection and Diagnosis of cancer is performed by self-examinations that play a pivotal role in identifying changes in moles or other abnormalities on the skin. Dermatologists conduct comprehensive examinations to detect potential skin cancers (13). In cases of suspicious lesions, a biopsy is performed to ascertain whether cancer is present.

Treatment modalities are tailored based on cancer type, size, and stage. Common interventions include surgery, radiation therapy, and the application of topical medications. Emphasizing the significance of early detection and intervention, the prognosis for skin cancer improves substantially. If concerns arise about skin changes, consulting a healthcare professional, ideally a dermatologist, is essential for a thorough evaluation. Additionally, adherence to sun-safe practices is fundamental in preventing skin cancer.

Research on skin cancer using computer-aided systems is essential for several reasons, as it offers numerous potential benefits and advancements within the dermatological field and healthcare (14). It can assist in the early detection and diagnosis of skin cancer. Earlier detection is vital for successful intervention and improved patient results. Automated systems can provide a high level of accuracy and precision in analyzing dermatoscopic images (15). This can enhance the reliability of diagnoses, lowering the possibility of false negatives and positives. Dermatological datasets, especially those containing a vast number of images, can be challenging to analyze manually (16). Computer-aided systems can efficiently handle large datasets, speeding up the diagnostic process. Automated systems provide an objective and standardized evaluation of skin lesions, minimizing the impact of subjectivity that may arise in manual assessments.

Computer-aided systems can serve as valuable tools to support dermatologists in their decision-making process (17). They can provide additional insights and information to aid healthcare professionals in making more informed diagnoses. Automated systems can be used for population-wide screening, allowing for the identification of individuals at risk and enabling early intervention strategies (18). This can be very valuable in areas with little access

Received: July 25, 2025

Volume 38 No. 3s, 2025
ISSN: 1311-1728 (printed version); ISSN: 1314-8060 (on-line version)

to healthcare resources. Research in this area contributes to the development and improvement of machine learning and artificial intelligence formulas for skin cancer detection. This continuous refinement enhances the performance and reliability of these systems over time. Early detection and accurate diagnosis through computer-aided systems can potentially reduce overall healthcare costs by preventing the progression of advanced skin cancers and the need for extensive treatments (19). Skin cancer is a global health concern (20). Research on computer-aided systems allows for the development of tools that can be applied worldwide, addressing the need for efficient and accessible diagnostic solutions. Advances in computer-aided systems contribute to the overall innovation in medical technology. This can pave the way for new and improved tools and methodologies in the broader area of imaging in medicine and diagnostics.

The research on skin cancer using computer-aided systems is not only necessary but also has a great deal of potential for revolutionizing the diagnosis and management of skin cancer, thereby improving patient results and advancements in healthcare practices.

The methodology proposed in this experimentation employ a hybrid approach considering the majority voting amongst XGBoost, FractalNet, and customized CNN models.

Studies in computer-aided dermoscopic image analysis usually consist of three primary phases: identifying the lesion's location, removing relevant characteristics of the lesion, and subsequently classifying it (21). Preprocessing techniques such are used by the researchers including adjustment of contrast (22), color balancing (23), normalization (24), and image calibration (25). These systems for computer-aided diagnostics are vital function-players in providing the supportive diagnostic system for experts through an accurate decision-making (26).

A six-step procedure is suggested for identifying melanomas by considering twenty-one preset standards for skin lesions (27). A two-stage approach was adopted, that demonstrated superior results compared to a single-stage approach for classification (28). These two methods offered a multi-stage approach and statistical analysis for the improvement of accuracy of diagnosis. The work for the detection of malignant melanomas was achieved with an 80% success rate by the artificial intelligence system (29). They also proposed the fuzzy Reasoning and multilevel neural networks lesions categorising (30). The efficacy of ANN in dermoscopic image analysis was worked on. The classification was compared with human experts for benign and malignant tumors (31). Support Vector Machine (SVM) and Feed-forward Network employed on 170 skin lesion images and achieved accuracies of 77% and 78% (32). The handmade elements were categorised with an accuracy of 92% for binary classification of cancerous and benign using linear regression and SVM (33). An accuracy of 93% was obtained by SVM with texture and color features for binary categories of skin lesions (34). This study is carried on the limited dataset samples.

Received: July 25, 2025

International Journal of Applied Mathematics

Volume 38 No. 3s, 2025

ISSN: 1311-1728 (printed version); ISSN: 1314-8060 (on-line version)

Consequently, deep learning gained its popularity in medical diagnosis, including diagnosis of cancer (35). Convolutional Neural Networks (CNNs) were extensively utilised in skin cancer diagnosis with medical image processing. An accuracy of 87% was obtained by CNN, which is commendable with melanoma classification.The dataset of 600 skin lesion samples was used for implementation (36). 81% accuracy was obtained with 1300 images of skin lesions (37). An ARL-CNN50 model was proposed and an accuracy of 85% was achieved for the skin cancer dataset (38). A hyper-connected CNN model was used for the classification of 1011 skin lesion images, and an accuracy of 74% was obtained (39). Improved performance of the model was observed with the use of data augmentation (40). Skin lesion categorisation was used using transfer learning (41). By using the transfer learning approach an accuracy of 78 % was achieved (42). The HAM10000 dataset was worked on, and an accuracy of 86% was achieved with the transfer learning technique (43). An Area Under Curve (AUC) showing sensitivity greater than 80% was attained with the pre-trained CNN model (44). Data augmentation performed with 2000 skin images of three classes and achieved an accuracy of 91.2% utilizing the FCRN deep convolutional neural network (45). Mobilenet, VGG-16, and a custom CNN model were employed, and 80% accuracy was attained across six different classes (46). With AlexNet and ResNet-18, achieved accuracies of 81% and 83% respectively over 2000 skin lesion images (47). An accuracy of 87% was reported for the binary classification with the employment of DenseNet and ResNet models averaging (48). Different pre-trained frameworks including InceptionResNetV2, SENet154, and InceptionV4 models were used, and the highest accuracy of 76% was achieved (49).

These findings collectively highlight the effectiveness and versatility of employing pre-trained models and transfer learning methodologies in enhancing accuracy in skin lesion classification studies.

Although different researchers contributed in the problem of skin cancer detection, there is requirement to improve The precision and additional metrics for performance. algorithms for deep learning and machine learning utilized for the study, including SOTA machine learning and deep learning models. Moreover, a new approach is necessary that utilizes the feature extraction capabilities of both machine and algorithms for deep learning. In this investigation, a hybrid approach is proposed comprising machine learning approach-XGBoost, and deep learning approaches- FractalNet and customized CNN. The majority voting is considered for the diagnosis decisions in the proposed approach.

Methodology

Images are utilized from HAM10000 dataset designed especially for the skin cancer detection. The dataset images are loaded into the proposed model. Initially data augmentation is performed which made the dataset samples balanced. Data balancing is necessary to train the model in an unbiased manner. If the data samples are imbalanced, the diagnosis decision could be partial towards the higher number of samples. Hence the augmentation is performed and number of samples in all the classes are made to be equal.

Received: July 25, 2025

International Journal of Applied Mathematics
Volume 38 No. 3s, 2025
ISSN: 1311-1728 (printed version); ISSN: 1314-8060 (on-line version)

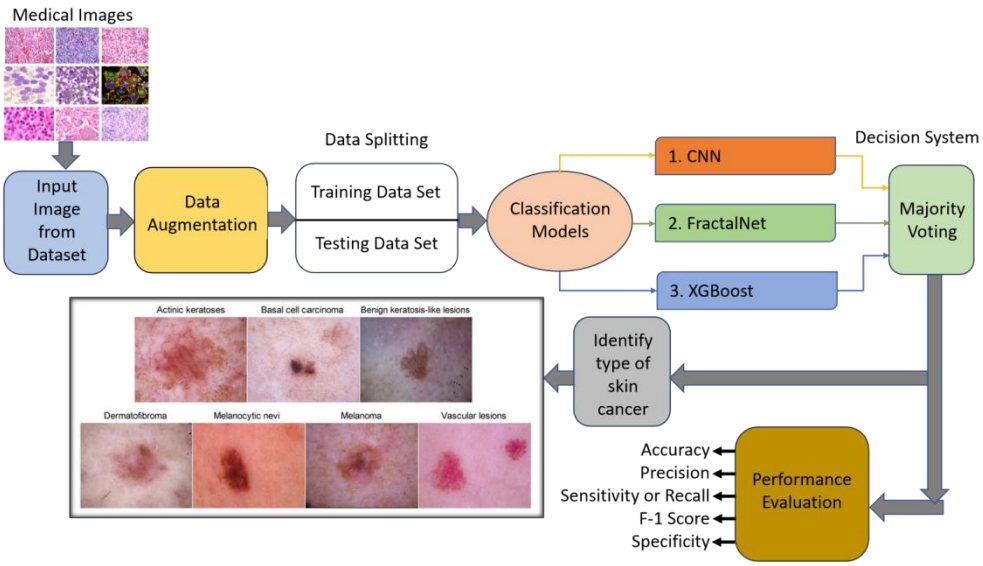

Figure 2: Proposed methodology

After the same, the three models are implemented, XGBoost, FractalNet and a customized CNN. These three models are placed in parallel and the diagnosis decision is done with majority voting between these models, as shown in figure 2. Following subsection explores these classification models:

Customized CNN

A Convolutional Neural Network (CNN) represents a category of deep learning models in particular crafted for image recognition and executing. Drawing inspiration from the human visual system, CNNs specialize in extracting hierarchical features from data using convolutional layers, which apply filters to input images, identifying patterns like edges and textures. Convolutional layers for downsampling, pooling layers for improved reasoning, and fully linked layers make up the conventional CNN architecture. Through convolutional operations, the network learns local features, while pooling layers diminish spatial dimensions to facilitate feature extraction. Employing learned parameters, CNNs autonomously and adaptively identify patterns, enabling tasks include object recognition and picture categorisation (50). Beyond image-related applications, CNNs find utility in diverse domains, including natural language processing, where hierarchical feature learning proves essential. The demonstrated effectiveness of CNNs across various fields underscores their versatility and capacity to discern intricate patterns within data (51). The Customized CNN architecture used in proposed methodology is shown in figure 3.

Received: July 25, 2025

International Journal of Applied Mathematics
Volume 38 No. 3s, 2025
ISSN: 1311-1728 (printed version); ISSN: 1314-8060 (on-line version)

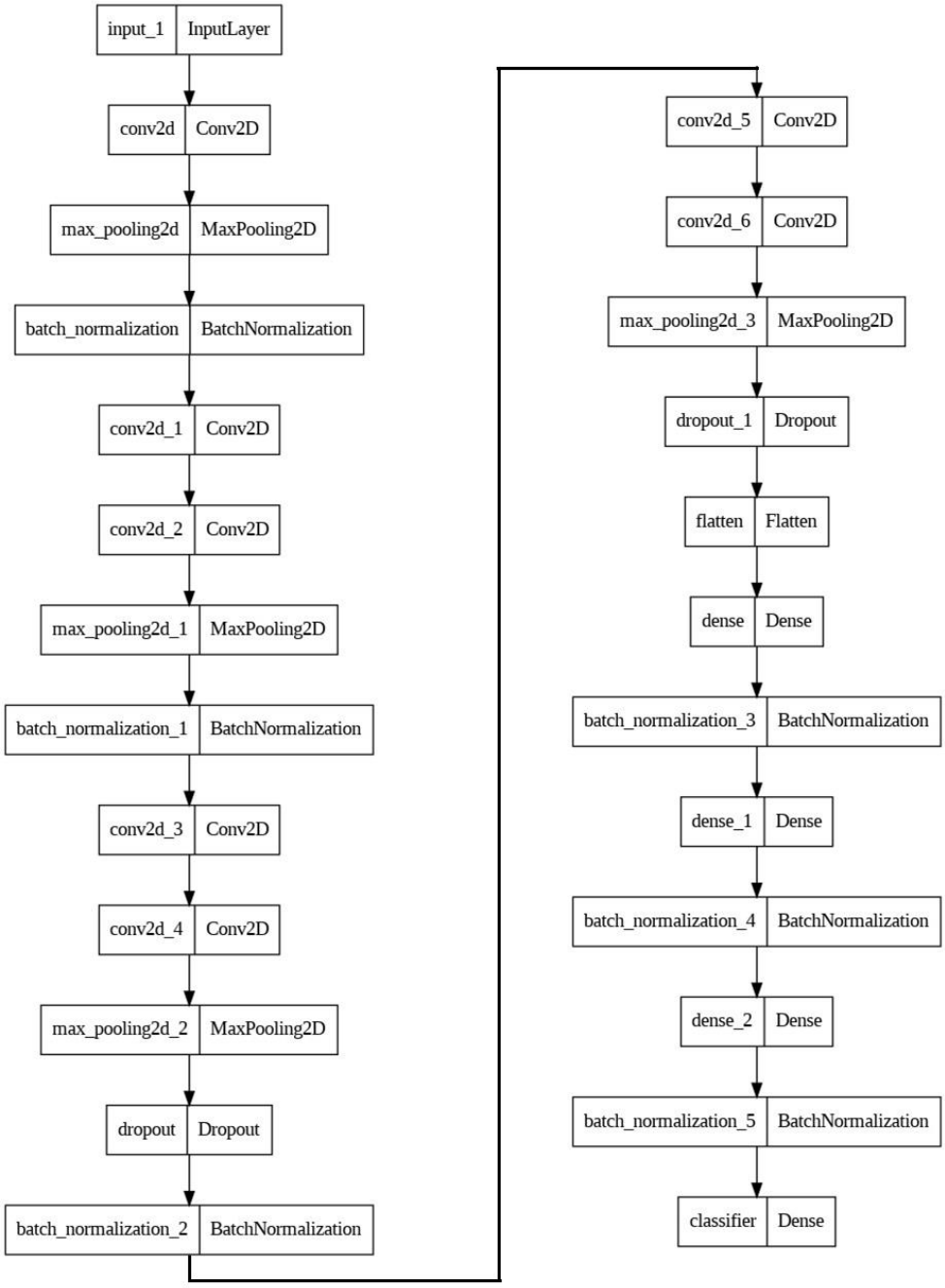

Figure 3: Customized CNN architecture

FractalNet

FractalNet constitutes an innovative neural network architecture designed to tackle the challenges associated with training highly intricate networks while concurrently upholding computational efficiency. Engineered to enhance the efficacy of convolutional neural networks (CNNs), FractalNet introduces a distinctive self-similar structure inspired by principles derived from fractal geometry. This departure from conventional CNNs involves

Received: July 25, 2025

International Journal of Applied Mathematics

Volume 38 No. 3s, 2025

ISSN: 1311-1728 (printed version); ISSN: 1314-8060 (on-line version)

the integration of reiterated fractal-like patterns, thereby enabling the construction of deep networks without incurring the anticipated rise in computational intricacy(52).

A pivotal innovation inherent to FractalNet lies in its capability to formulate each layer as a synthesis of self-replicating sub-blocks that mirror the overarching structure of the entire network. These sub-blocks, reminiscent of fractal patterns, demonstrate consistent structures across varying scales. This inherent self-similarity empowers the model to proficiently assimilate features at multiple levels of abstraction, thereby facilitating the representation of intricate patterns within datasets.

One of the primary merits distinguishing FractalNet from other CNN models lies in its heightened proficiency in capturing hierarchical features. Conventional deep networks grapple with challenges during training, such as issues like vanishing gradients or information bottlenecks within exceptionally deep architectures. FractalNet adeptly mitigates these challenges by judiciously harnessing self-similar structures, thereby fostering a more effective flow of information throughout the network.

Furthermore, the self-similar architecture of FractalNet engenders heightened computational efficiency. Despite its augmented depth, FractalNet sidesteps the anticipated exponential surge in computational requisites often associated with deep networks. This attribute renders it particularly appealing in scenarios where computational resources are constrained.

The self-replicating nature of FractalNet also fosters a more modular and scalable network design. The embedded fractal patterns facilitate seamless extensions or customizations to the model, imparting flexibility in adapting the architecture to distinct tasks or datasets (53).

It epitomizes a pioneering paradigm in deep neural network architecture, leveraging self-similar structures inspired by fractal geometry. Its superiority over other CNN models is underscored by its adeptness in efficiently capturing hierarchical features, alleviating training challenges in profoundly deep networks, preserving computational efficiency, and furnishing a scalable and modular design. These attributes collectively position FractalNet as a compelling advancement in the domain of deep learning architectures, with broad potential applications across diverse domains.

The detail architecture of FractalNEt is shown in Figure 4. The essential component of FractalNet is a self-replicating sub-block that mirrors the total network structure as a whole. These sub-blocks, resembling fractal patterns, maintain a consistent structure across different scales. This self-similarity enables the model to efficiently learn features at multiple levels of abstraction, facilitating the representation of complex patterns within data. One noteworthy benefit of FractalNet is its enhanced the capacity to capture hierarchical features. In contrast to conventional deep networks that may face challenges like vanishing gradients or information bottlenecks in very deep architectures, FractalNet addresses these issues by leveraging self-similar structures. This results in a more effective flow of information throughout the network. Despite its increased depth, FractalNet maintains computational efficiency, avoiding the exponential growth in computational requirements typically

Received: July 25, 2025

International Journal of Applied Mathematics

Volume 38 No. 3s, 2025

ISSN: 1311-1728 (printed version); ISSN: 1314-8060 (on-line version)

associated with deep networks (54). This efficiency makes it particularly appealing in scenarios where computational resources are limited.

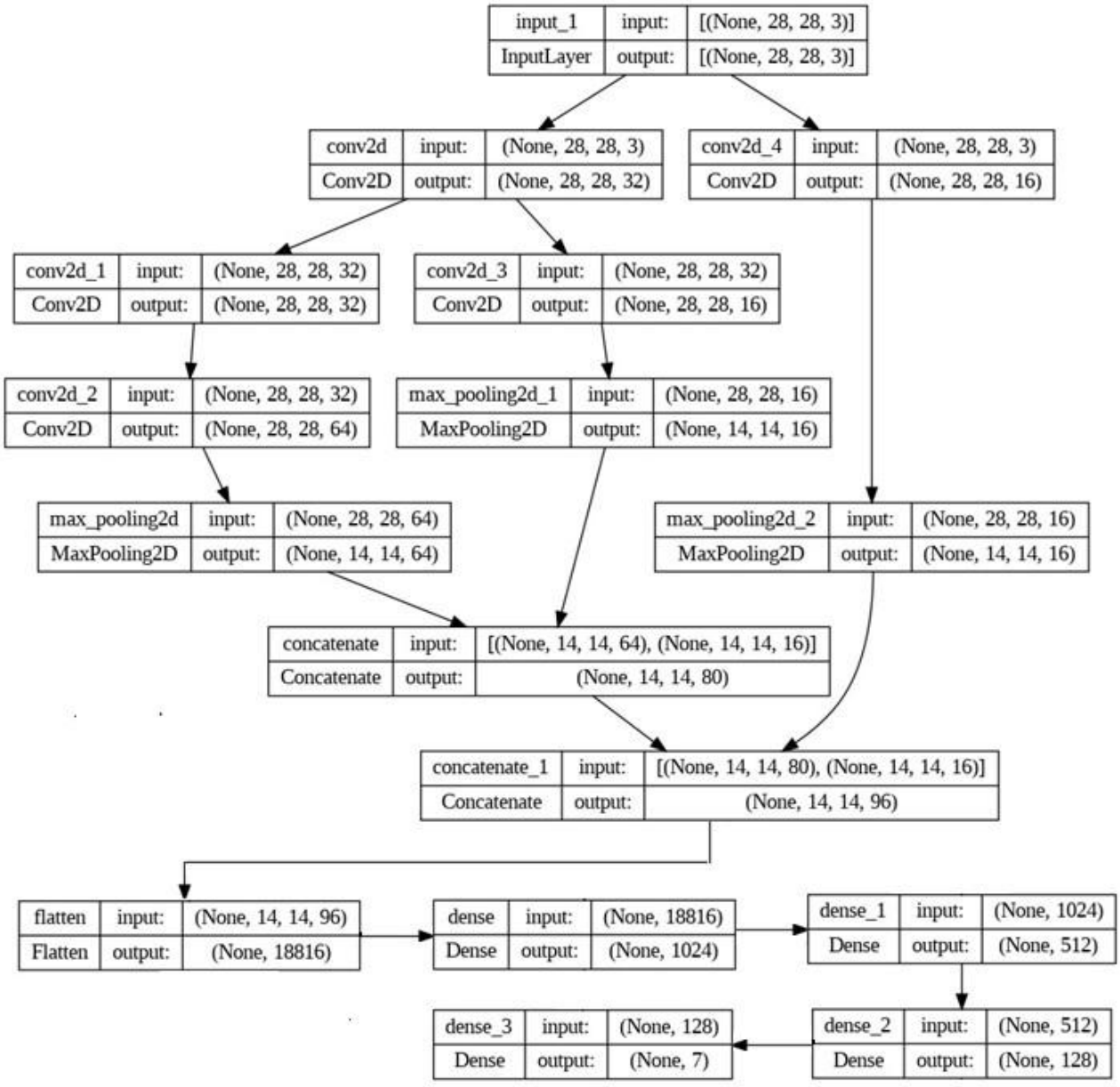

Figure 4: FractalNet architecture

Let V shows the index of truncated fractal $f_V(.)$. A single convolution network is considered to be the base case.

$$f_1(y) = conv\,(y) \qquad [1]$$

Then recursively the other successive fractals can be explained as in equation 2

$$f_{V+1}(y) = [(f_V \circ f_V)(y)] \oplus [conv(y)] \qquad [2]$$

Received: July 25, 2025

International Journal of Applied Mathematics

Volume 38 No. 3s, 2025

ISSN: 1311-1728 (printed version); ISSN: 1314-8060 (on-line version)

where $^{\circ}$ is the composition and $\oplus$ shows the join operation. According to Figure 4, V correlates to the network's breadth or number of columns $f_V(.)$. Number of layers of convolution defines the depth considered to be Scales as the distance along the longest path from input to output $2^{(V+1)}$. Two feature blobs which are the result of the *conv* layers, are merged by using join operation, $\oplus$. The quantity of channels corresponds to the filter set's size in the previous convolution layer. When the fractal grows, adjacent connects are collapsed as seen on the right side of Figure 4, into a single connect layer spanning many columns. A single output blob is created by the join layer by combining all of the input feature blobs.

XGBoost

XGBoost, which denotes Extreme Gradient Boosting, represents a highly influential an algorithm for machine learning widely utilized for regression and classification tasks. Developed by Tianqi Chen, this algorithm has gained considerable traction owing to its exceptional predictive capabilities. At its core, XGBoost operates as an ensemble learning method, combining predictions from multiple weak learners, predominantly gradient boosted decision trees (55).

A distinctive feature of XGBoost is its implementation of gradient boosting, wherein successive models are added to rectify errors made by preceding models. This iterative process continues until a predetermined number of trees are generated or until further improvements in predictive accuracy become negligible.

To prevent overfitting, XGBoost integrates regularization techniques, incorporating penalty terms into the loss function (56). This makes the model want to becoming excessively intricate and enhances its generalization to unseen data. The algorithm optimizes an objective function, a composite involving a regularisation term and a loss function, with the flexibility to select several objective procedures according to the particular assignment, be it binary classification, multiclass classification, or regression. An intrinsic feature of XGBoost is its ability to assess feature importance. By evaluating the contribution of each feature to predictive performance, the algorithm facilitates insights into influential variables and aids in feature selection. Notably, it is designed for efficiency and speed, supporting parallel and distributed computing. It also implements tree pruning to restrict tree depth during construction, finding a middle ground between computational efficiency and model complexity.

XGBoost is a versatile and effective machine learning algorithm with a solid reputation for accuracy, scalability, and flexibility (57). Its ensemble learning approach, gradient boosting technique, regularization methods, and feature importance evaluation collectively contribute to its widespread adoption and success across diverse domains.

XGBoost algorithm has some important mathematics including learning objective, gradient tree boosting, and split finding algorithms.

Received: July 25, 2025

International Journal of Applied Mathematics

Volume 38 No. 3s, 2025

ISSN: 1311-1728 (printed version); ISSN: 1314-8060 (on-line version)

Regularized Learning Objective:

Consider n instances and m characteristics in a data collection$\mathcal{D} = \{(\mathbf{x}_i, y_i)\}(|\mathcal{D}| = n, \mathbf{x}_i \in \mathbb{R}^m, y_i \in \mathbb{R})$, An ensemble model of trees considered to have K additive functions to forecast the result.

$$\hat{y}_i = \phi(\mathbf{x}_i) = \sum_{k=1}^{K} f_k(\mathbf{x}_i),\ f_k \in \mathcal{F} \qquad [3]$$

where $\mathcal{F} = \{f(\mathbf{x}) = w_{q(\mathbf{x})}\}(q: \mathbb{R}^m \to T, w \in \mathbb{R}^T)$ is the regression tree space, sometimes referred to as CART. Here, T is the number of leaves in the tree, and q represents the structure of each tree that translates each example to the associated leaf index. Each f_k corresponds to an independent tree structure q and leaf weights w.

Regression trees differ from decision trees in that each leaf has a continuous score, denoted by w_i, which represents the score on the i-th leaf. To get the final prediction, for instance, one may use the decision rule in the trees (provided by q) to categorise it into the leaves and then add up the scores in the appropriate leaves (supplied by w). Minimise the following regularised goal in order to understand the set of functions utilised in the model:

$$\mathcal{L}(\phi) = \sum_i l(\hat{y}_i, y_i) + \sum_k \Omega(f_k) \qquad [4]$$

$$\text{where } \Omega(f) = \gamma T + \frac{1}{2}\lambda \parallel w\parallel^2$$

In this case, the difference between the goal y_i and the forecast y ˆ_i is measured by the differentiable convex loss function, l. The complexity of the model, or the regression tree functions, is penalised by the second factor, Ω. The extra regularisation period aids in preventing over-fitting by smoothing the final learning weights.

Gradient Tree Boosting:

Since functions are used as parameters in the tree ensemble model in Eq. (4), conventional optimisation techniques cannot be applied in Euclidean space. Rather, the model receives training in an additive fashion. Formally, let y ˆ_i^((t)) represent the prediction of the i-th occurrence at the t-th iteration; in order to minimise the subsequent goal, f_t must be added.

$$\mathcal{L}^{(t)} = \sum_{i=1}^{n} l\left(y_i, \hat{y}_i{}^{(t-1)} + f_t(\mathbf{x}_i)\right) + \Omega(f_t) \qquad [5]$$

This means the f_t is added greedily that most enhances the model in line with to Eq. (4).

In the generic scenario, the aim may be easily optimised by using the second-order approximation (12).

Received: July 25, 2025

International Journal of Applied Mathematics

Volume 38 No. 3s, 2025

ISSN: 1311-1728 (printed version); ISSN: 1314-8060 (on-line version)

$$\mathcal{L}^{(t)} \simeq \sum_{i=1}^{n} \left[l\left(y_i, \hat{y}^{(t-1)}\right) + g_i f_t(\mathbf{x}_i) + \frac{1}{2} h_i f_t^2(\mathbf{x}_i) \right] + \Omega(f_t) \qquad [6]$$

where $g_i = \partial_{\hat{y}^{(t-1)}} l\left(y_i, \hat{y}^{(t-1)}\right)$ and $h_i = \partial^2_{\hat{y}^{(t-1)}} l\left(y_i, \hat{y}^{(t-1)}\right)$ are gradient statistics on the loss function of the first and second order. At step t, the following simplified goal could be achieved by eliminating the constant term.

$$\tilde{\mathcal{L}}^{(t)} = \sum_{i=1}^{n} \left[g_i f_t(\mathbf{x}_i) + \frac{1}{2} h_i f_t^2(\mathbf{x}_i) \right] + \Omega(f_t) \qquad [7]$$

Define $I_j = \{i | q(\mathbf{x}_i) = j\}$ as leaf j's instance set. We can expand Ω in the following way to rephrase Eq (5):

$$\tilde{\mathcal{L}}^{(t)} = \sum_{i=1}^{n} \left[g_i f_t(\mathbf{x}_i) + \frac{1}{2} h_i f_t^2(\mathbf{x}_i) \right] + \gamma T + \frac{1}{2} \lambda \sum_{j=1}^{T} w_j^2 \qquad [8]$$

For a fixed structure $q(\mathbf{x})$, we can compute the optimal weight w_j^* of leaf j by

$$w_j^* = -\frac{\sum_{i \in I_j} g_i}{\sum_{i \in I_j} h_i + \lambda} \qquad [9]$$

and determine the matching ideal value by

$$\tilde{\mathcal{L}}^{(t)}(q) = -\frac{1}{2} \sum_{j=1}^{T} \frac{\left(\sum_{i \in I_j} g_i \right)^2}{\sum_{i \in I_j} h_i + \lambda} + \gamma T \qquad [8]$$

A tree structure q's quality may be evaluated using a scoring function derived from equation (6). Although it is calculated for a larger range of objective functions, this score is similar to the impurity score used to assess decision trees.

Typically, listing every conceivable tree structure q is not feasible. Instead, a greedy method is employed, which begins with a single leaf and builds the tree's branches repeatedly. Let's assume that the instance sets of the left and right nodes following the split are I_L and I_R. If we assume I=I_LUI_R, the loss reduction following the split is provided by

$$\mathcal{L}_{split} = \frac{1}{2} \left[\frac{\left(\sum_{i \in I_L} g_i\right)^2}{\sum_{i \in I_L} h_i + \lambda} + \frac{\left(\sum_{i \in I_R} g_i\right)^2}{\sum_{i \in I_R} h_i + \lambda} - \frac{\left(\sum_{i \in I} g_i\right)^2}{\sum_{i \in I} h_i + \lambda} \right] - \gamma \qquad [10]$$

Received: July 25, 2025

International Journal of Applied Mathematics

Volume 38 No. 3s, 2025

ISSN: 1311-1728 (printed version); ISSN: 1314-8060 (on-line version)

Performance Metrics

Classification of normal and abnormal cell images and the multi-class classification are the prime motivation of the presented work. There are different metrics employed for the evaluation of the performance of the proposed system. Following are the parameters utilized for accuracy measurement (58,59,60,61,62):

Accuracy : $Accuracy = \frac{TP+TN}{TP+TN+FP+FN}$ [11]

Where TP=true positive, TN=true negative, FP=false positive, FN=false negative

Recall : $Recall = \frac{TP}{TP+FN}$ [12]

Precision : $Precision = \frac{TP}{TP+FP}$ [13]

F1-score : $F1 - Score = 2 * \frac{Precision*Recall}{Precision+Recall}$ [14]

Specificity:

Specificity serves as an indicator of performance in machine learning scenarios involving binary classification. This metric evaluates the model's proficiency in accurately recognizing instances belonging to the negative class, commonly denoted as "true negatives," among all the genuine negative instances. Essentially, specificity gives an indication of how effectively the model avoids misclassifying negative instances, contributing valuable insights into its ability to correctly identify non-target outcomes. It is given by the equation below.

$Specificity = \frac{TN}{TN+FP}$ [15]

Confusion matrix :

To show classifier performance based on the four parameters (TP, FP, TN, and FN) mentioned above, a confusion matrix is frequently utilised. A confusion matrix is created when these are placed against one another.

Dataset

The HAM10000 dataset, denoting "Human against Machine with 10000 training images," functions as a valuable asset within the domain of dermatology. In particular curated to propel research endeavors in the evolution and evaluation of machine learning methods for identifying and categorising skin cancer, This dataset is an essential tool for advancing scientific exploration on the terrain (63).

It comprises of a total based on 10,015 dermatoscopic pictures that meticulously capture pigmented skin lesions, the HAM10000 dataset is used in a diverse and useful tool for in - depth analysis. This dataset meticulously categorizes images into seven different categories of diagnosis, covering melanoma, nevus, basal cell carcinoma, actinic keratosis, benign keratosis, dermatofibroma, and vascular lesions. Originating from collaborative efforts

Received: July 25, 2025

International Journal of Applied Mathematics

Volume 38 No. 3s, 2025

ISSN: 1311-1728 (printed version); ISSN: 1314-8060 (on-line version)

between researchers at the Medical University of Vienna, Austria, this dataset uniquely combines medical and technological expertise. The primary objective in creating the HAM10000 dataset is to bolster and streamline research initiatives in the field of computer-aided diagnostic (CAD) systems, ultimately aiming to improve the precision and efficiency of skin cancer detection. At the core of the dataset are dermatoscopic images, crucial components of dermatology examinations, captured using dermatoscopes—specialized handheld devices with integrated lighting and magnification capabilities, ensuring a detailed and comprehensive representation. Recognizing the intricate nature of skin cancer diagnosis, the HAM10000 dataset provides a thorough compilation of images that authentically mirror the complexities encountered in real-world diagnostic scenarios (64).

Melanocytic nevi, encompassing a diverse array of benign neoplasms originating from melanocytes, exhibit various dermatoscopic perspectives within our dataset, comprising 6705 images. Melanoma, a cancerous tumour originating from melanocytes, manifests in distinct variants, with 1113 images covering both invasive and non-invasive (in situ) forms. Excluded are non-pigmented, subungual, ocular, or mucosal melanomas. The "Benign Keratosis" category consolidates seborrheic keratoses, solar lentigo, and lichen-planus like keratoses (LPLK), totaling 1099 images. Although these subgroups may present diverse dermatoscopic features, they are grouped together due to biological similarities, despite morphological challenges such as melanoma-like features in LPLK. Epithelial skin cancer frequently manifests as basal cell carcinoma with various morphologic presentations, contributes 514 images. 327 photos show the prevalent non-invasive forms of squamous cell carcinoma, actinic keratoses (also known as solar keratoses) and intraepithelial carcinoma (also known as Bowen's disease). Haemorrhages and vascular skin lesions, such as cherry angiomas, angiokeratomas, and pyogenic granulomas, are encompassed in 142 images. Dermatofibroma, a benign skin lesion demonstrating brown pigmentation and often featuring a central fibrotic zone, is portrayed in 115 images. This comprehensive categorization aims to facilitate nuanced research in dermatology, offering a rich dataset that captures the intricacies of skin lesions from diverse perspectives.

Results

Initially, data balancing was necessary during this experimentation, as the decision might be biased when it dataset contain the unbalanced samples. Figure 5 shows the graphical representation of dataset samples before and after data augmentation. After the augmentation, all the classes in the dataset were made the equal sized samples as show in Figure 5 (B). These samples are loaded in the proposed models and the measures for performance were acquired. Following subsection explores the details of the outcomes.

Received: July 25, 2025

International Journal of Applied Mathematics

Volume 38 No. 3s, 2025

ISSN: 1311-1728 (printed version); ISSN: 1314-8060 (on-line version)

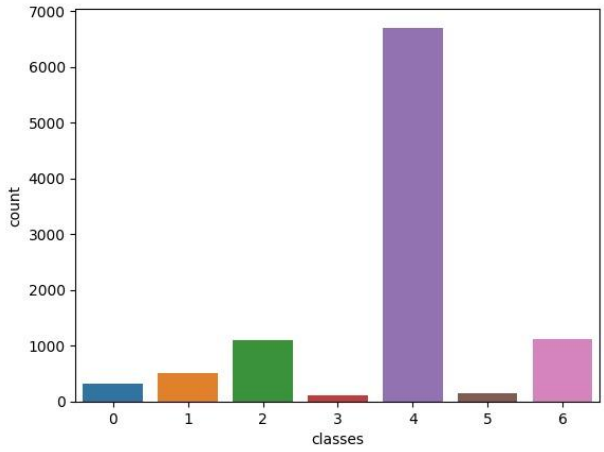

(A)

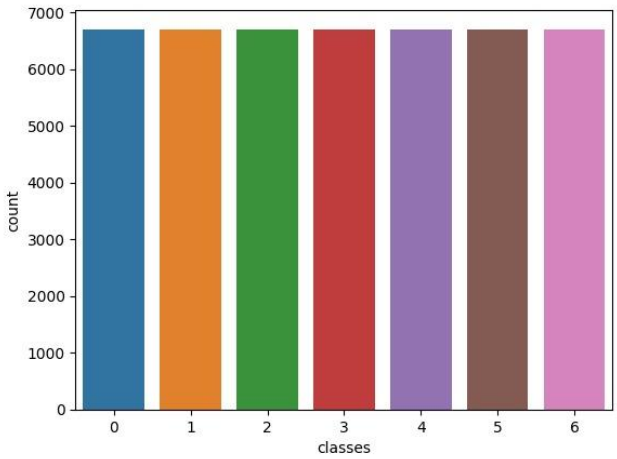

(B)

Figure 5: (A) Original data (B) Balanced data

XGBoost

Figure 6 displays the confusion matrix with XGBoost as classifier and Table 1 displays the precise performance data for each class. Recall, F1-score, specificity, and accuracy.

Received: July 25, 2025

International Journal of Applied Mathematics

Volume 38 No. 3s, 2025

ISSN: 1311-1728 (printed version); ISSN: 1314-8060 (on-line version)

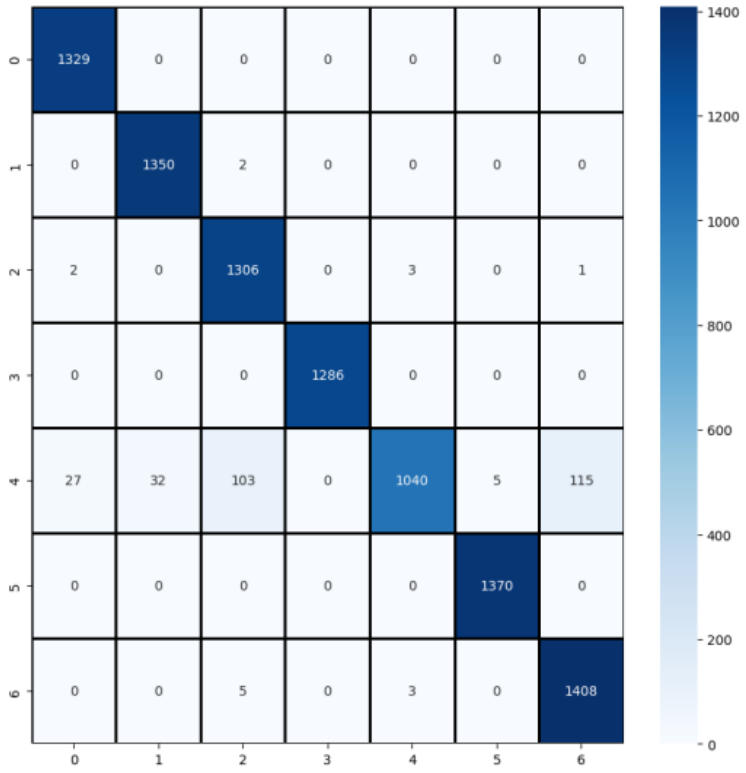

Figure 6: Confusion Matrix with XGBoost Classifier

The values of these measures obtained with XGBoost are 97%, 96.79%, 96.69%, and 16.49% for precision, recall F-score and specificity with the accuracy of 96.83 %. Table 1 explains the performance measures for the XGBoost classifier.

Table 1: Performance measures of XGBoost classifier

Class	Precision	Recall	F1-Score	Specificity	Support
0	97.86%	100%	98.22%	0.0%	1329
1	97.68%	99.85%	98.76%	05.88%	1352
2	92.23%	99.54%	95.75%	05.17%	1312
3	100%	100%	100%	0.0%	1286
4	99.43%	78.67%	87.84%	97.92%	1322
5	99.64%	100%	99.82%	0.0%	1370
6	92.39%	99.44%	95.78%	06.45%	1416
Macro Average	**97.03%**	**96.79%**	**96.69%**	**16.49%**	**9387**
Weighted Average	97.00%	96.83%	96.70%	--	9387
Accuracy	**96.83 %**				

Received: July 25, 2025

International Journal of Applied Mathematics

Volume 38 No. 3s, 2025

ISSN: 1311-1728 (printed version); ISSN: 1314-8060 (on-line version)

CNN

A customized CNN is implemented and the dataset is passed through the model to get different performance measures. Figure 7 displays the validation loss, training, and training, validation accuracies with a total of 40 epochs.

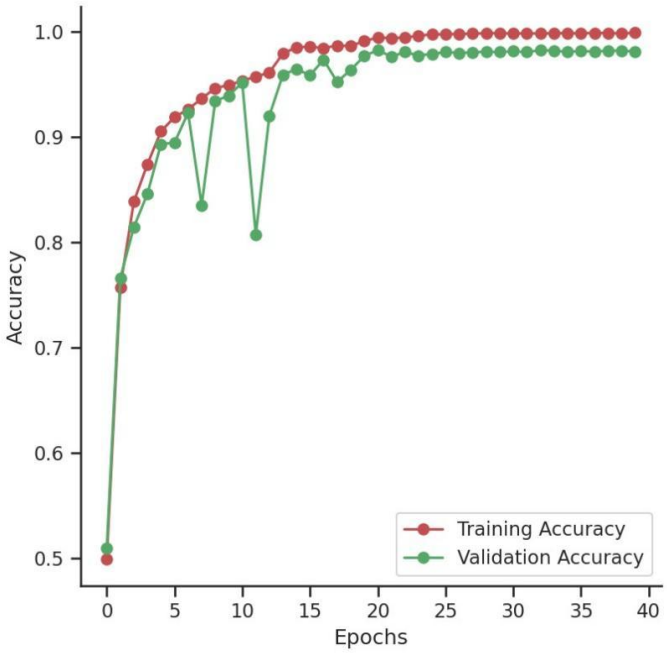

(A)

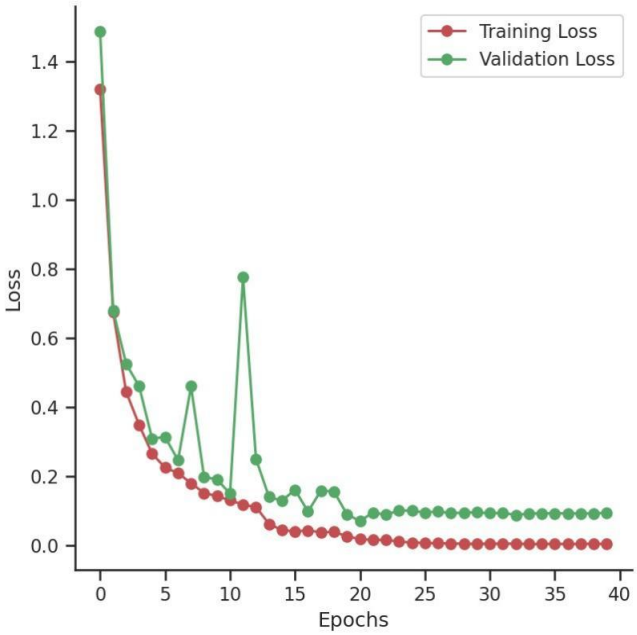

(B)

Figure 7: (A) Training and Validation Loss curve for 40 epochs (B) Training and validation accuracy curve for 40 epochs

Received: July 25, 2025

International Journal of Applied Mathematics

Volume 38 No. 3s, 2025

ISSN: 1311-1728 (printed version); ISSN: 1314-8060 (on-line version)

Figure 8 explores the classification with the help of confusion matrix. It displays the expected and actual number of samples for the entire dataset.

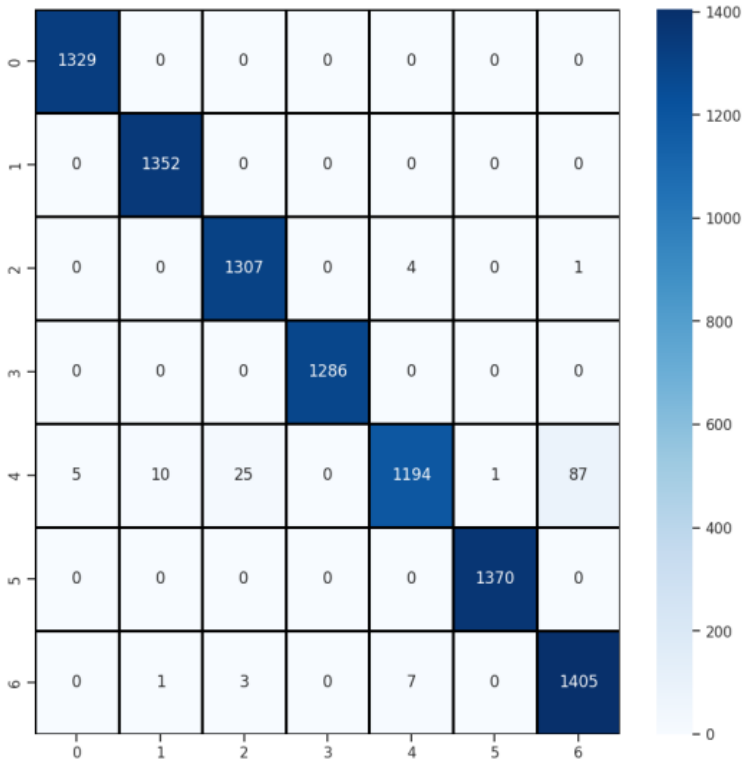

Figure 8: Confusion matrix for CNN classifier

Table 2 explains the performance measures for the customized CNN as the classifier for six different classes of the dataset. Precision, recall, F-score, specificity and accuracy values obtained with this classifier are 98.51%, 98.45%, 98.46%, 16.91%, and 98.47% respectively.

Table 2: Performance measures of CNN classifier

Class	Precision	Recall	F1-Score	Specificity	Support
0	99.63%	100%	99.81%	0.0%	1329
1	99.19%	100%	99.59%	0.0%	1352
2	97.90%	99.62%	98.75%	15.15%	1312
3	100%	100%	100%	0.0%	1286
4	99.09%	90.32%	94.50%	92.09%	1322
5	99.93%	100%	99.96%	0.0%	1370
6	94.11%	99.22%	96.60%	11.11%	1416
Macro Average	**98.55%**	**98.45%**	**98.46%**	**16.91%**	**9387**
Weighted Average	98.51%	98.47%	98.45%	--	9387
Accuracy	**98.47 %**				

Received: July 25, 2025

International Journal of Applied Mathematics
Volume 38 No. 3s, 2025
ISSN: 1311-1728 (printed version); ISSN: 1314-8060 (on-line version)

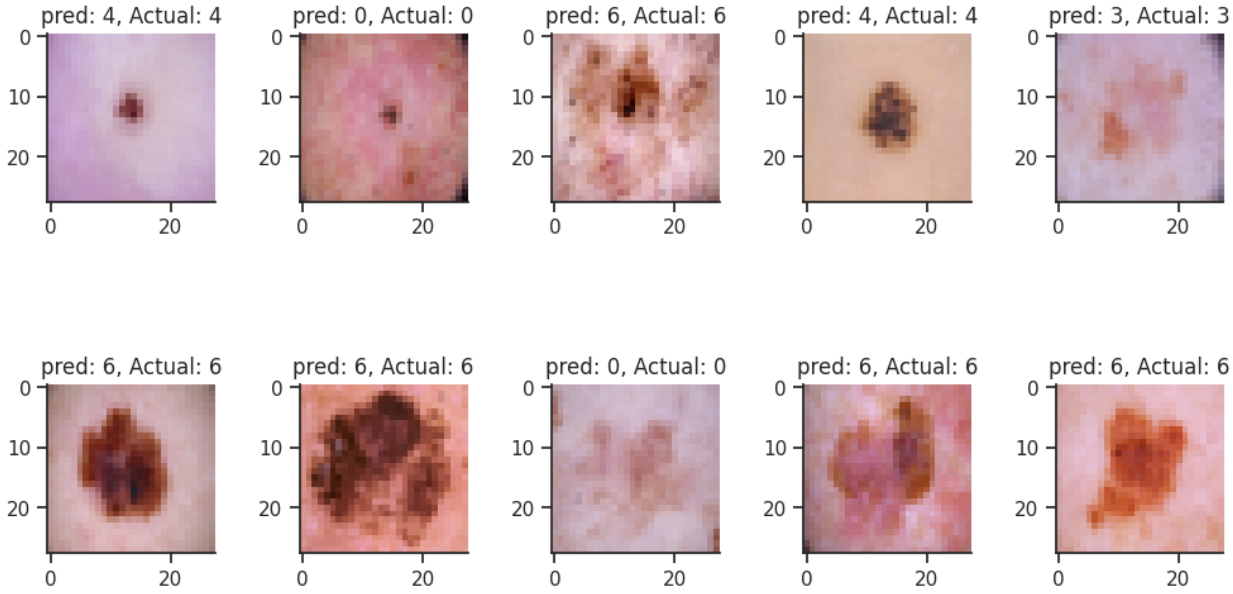

Figure 9: Actual and Predicted output images

Figure 9 shows the actual and predicted images by utilizing the CNN model.

FractalNet

Figure 10 explores the arrangement of different categories in the dataset with the confusion matrix. This is accustomed to get the actual and predicted values of the dataset samples.

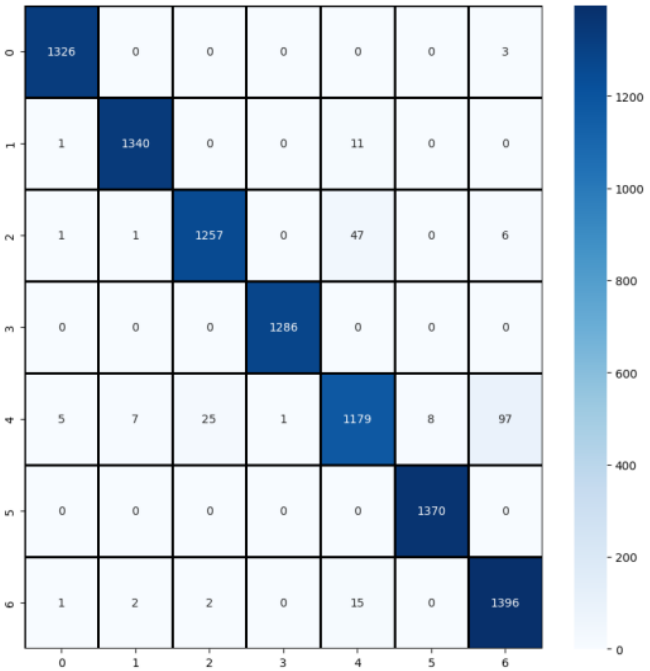

Figure 10: Confusion matrix with FractalNet classifier

Table 3 gives the performance measures precision, recall, F-score, specificity, and accuracy as 97.53%, 97.52%, 97.59%, 33%, and 97.52 % respectively.

Received: July 25, 2025

International Journal of Applied Mathematics
Volume 38 No. 3s, 2025
ISSN: 1311-1728 (printed version); ISSN: 1314-8060 (on-line version)

Table 3: Performance measures of FractalNet classifier

Class	Precision	Recall	F1-Score	Specificity	Support
0	99.60%	99.77%	99.59%	27.27%	1329
1	99.26%	99.11%	99.19%	54.55%	1352
2	97.90%	95.81%	96.84%	67.07%	1312
3	99.92%	100%	99.96%	0.0%	1286
4	94.17%	89.18%	91.61%	66.20%	1322
5	99.42%	100%	99.71%	05.00%	1370
6	92.94%	98.59%	95.68%	15.87%	1416
Macro Average	**97.57%**	**97.50%**	**97.51%**	**33.00%**	9387
Weighted Average	97.53%	97.52%	97.50%	--	9387
Accuracy	**97.52 %**				

Hybrid Model

After the individual models' evaluation, an hybrid model is implemented consisting of all these three models, XGBoost, CNN, and FractalNet. Figure 11 shows the confusion matrix with the utilization of proposed hybrid model showing the actual and predicted samples of the dataset.

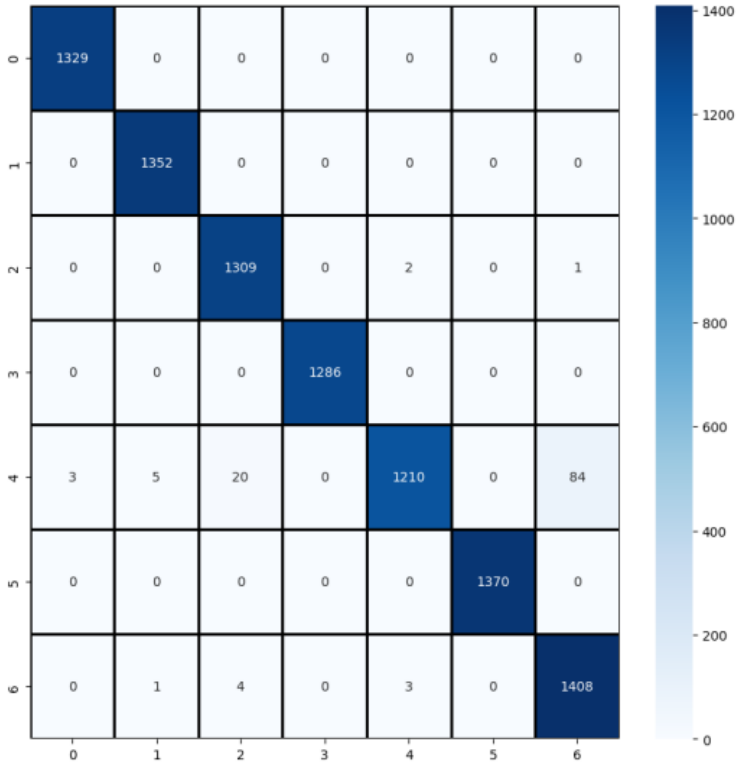

Figure 11: Confusion matrix with hybrid model and voting approach

Received: July 25, 2025

International Journal of Applied Mathematics

Volume 38 No. 3s, 2025

ISSN: 1311-1728 (printed version); ISSN: 1314-8060 (on-line version)

Table 4 explains the different performance measures with using a hybrid model that is based on majority voting approach. The values of precision, recall, F-score, specificity, and accuracy are obtained as 98.74%, 98.69%, 98.68%, 16.49%, and 98.69 % respectively. These values shown the improvement of these parameters with majority voting hybrid approach.

Table 4: Performance measures of hybrid classifier

Class	Precision	Recall	F1-Score	Specificity	Support
0	99.77%	100%	99.89%	0.0%	1329
1	99.56%	100%	99.78%	0.0%	1352
2	98.20%	99.77%	98.98%	11.11%	1312
3	100%	100%	100%	0.0%	1286
4	99.59%	91.53%	95.39%	95.73%	1322
5	100%	100%	100%	0.0%	1370
6	94.31%	99.44%	96.80%	08.60%	1416
Macro Average	**98.78%**	**98.68%**	**98.69%**	**16.49%**	9387
Weighted Average	98.74%	98.69%	98.68%	--	9387
Accuracy	**98.69 %**				

Comparison with state-of-the-art

Table 5 shows the comparison of the proposed method with the state-of-the-art proposed by different researcher for the same problem. As seen from the table accuracy is considered the comparison metric. The accuracies obtained by different researchers is from 66.2 % to 93.5 %. Moreover, the proposed method utilized XGBoost, CNN, and FractalNet combination obtained the accuracy of 98.69 % which is good as compared to the state-of-the-art proposed by the researchers shown in Table 5.

Table 5: Performance measures of hybrid classifier

Reference	Method	Accuracy (%)
(65)	CNN+GoogleLeNet	86.7
(66)	Dep ResNet +UNet	76
(67)	MobileNet +Efficient B7	88.3
(68)	CNN+ANN	84.2
(69)	VGG13 + MetaNet	66.2
(70)	MobileNet-V2 + Spiking Neural Net	89.8
(71)	CNN+ Fuzzy K-means	92.5

Received: July 25, 2025

International Journal of Applied Mathematics

Volume 38 No. 3s, 2025

ISSN: 1311-1728 (printed version); ISSN: 1314-8060 (on-line version)

(72)	DCNN	90.16
(73)	VGG16 + ResNet + CapsNet	93.5
Proposed Method	**XGBoost + CNN + FractalNet**	**98.69**

Discussion

Skin cancer is becoming more common over time and it has grown in number to become the most dominant type of cancer across the globe. The major contributing factor of skin cancer is excessive exposure to sunlight or sunlamps. UV light is bad for the skin because it damages the skin cell's DNA. As a result, skin cells undergo mutations that lead to unregulated cell division and cancerous growths. The importance of detecting skin cancer at an early stage cannot be overstated.Within the suggested work, a hybrid system is presented that utilizes the three frameworks, XGBoost, FractalNet, and a customized CNN. The majority voting is considered during the decision of diagnosis of different classes defining the type of the skin cancer.

The system performance is evaluated by using different performance measures. Precision stands out as a critical metric for assessing classification results, representing the ratio of true positive predictions to all positive predictions generated by the model during testing. The value of precision obtained by XGBoost, FractalNet, CNN, and hybrid model are 97%, 98.51%, 97.53%, and 98.74% respectively. Similarly, recall holds significance, providing the proportion of positive predictions from an experiment in relation to true positives and false negatives. Ideally, a recall value approaching 1 ensures minimal occurrences of false negatives in predictions. The recall values obtained by XGBoost, FractalNet, CNN, and hybrid model are 96.83%, 98.47%, 97.52%, and 98.69% respectively. The F1-score metric is an essential measure in assessing the deep learning and machine learning models' performance. Recognizing the inherent trade-off between precision and recall, the F1-score serves as a balanced metric, representing the harmonic mean of precision and recall. This comprehensive measure addresses both false positives and false negatives, providing a holistic evaluation of model performance. The value of F-score obtained by XGBoost, FractalNet, CNN, and hybrid model are 96.7%, 98.45%, 97.5%, and 98.68% respectively. In the realm of medical diagnostics and classification models, specificity assumes importance. It gauges the model's accuracy in accurately determining true negative cases among all actual negative cases, reflecting its ability to precisely discern individuals or instances lacking a specific condition or characteristic. The values of specificity obtained by XGBoost, FractalNet, CNN, and hybrid model are 16.49%, 16.91%, 33%, and 16.49% respectively. An additional crucial parameter in Accuracy is the criterion for assessing model performance, quantifying the proportion of accurate forecasts to the total number of predictions made.

Received: July 25, 2025

International Journal of Applied Mathematics

Volume 38 No. 3s, 2025

ISSN: 1311-1728 (printed version); ISSN: 1314-8060 (on-line version)

Together, these measures provide a thorough evaluation of the effectiveness and reliability of machine learning and deep learning models. The value of precision obtained by XGBoost, FractalNet, CNN, and hybrid model are 96.83 %, 98.47%, 97.52 %, and 98.69 % respectively.

Integrating XGBoost, FractalNet, and Convolutional Neural Networks (CNNs) simultaneously through a majority voting strategy presents numerous advantages for classification endeavors. Each model (XGBoost, FractalNet, and CNN) possesses distinct strengths and weaknesses in grasping various facets of the data. The amalgamation of these models facilitates a more holistic comprehension of features, potentially leading to heightened accuracy and resilience in classification tasks. XGBoost excels in handling structured/tabular data, FractalNet introduces self-similar structures for hierarchical feature learning, and CNNs are adept at capturing spatial hierarchies in image data. Integrating these diverse models provides a more comprehensive range of feature representation, accommodating the diverse characteristics of the data. The fusion of models with diverse underlying architectures creates an ensemble that leverages the strengths of each individual model. This synergy has the potential to enhance overall predictive performance. Combining models with different characteristics aids in mitigating overfitting. If one model tends to overfit to specific patterns or noise in the data, the ensemble's voting mechanism can counterbalance these effects, resulting in more generalized outcomes. The majority voting approach fosters a collaborative decision-making process. Consensus among multiple models in a classification instills greater confidence in the predicted label, potentially reducing the impact of outliers or noisy instances. XGBoost's suitability for structured data, FractalNet's proficiency in hierarchical feature learning, and CNNs' effectiveness with image data contribute to the ensemble's adaptability across a diverse array of datasets and data types. Incorporating improvements or updates to any individual model (XGBoost, FractalNet, or CNN) into the ensemble is seamless, requiring minimal restructuring of the system. The deep learning architectures of FractalNet and CNNs enable the capture of intricate relationships within the data. Simultaneously, XGBoost's proficiency in handling non-linear relationships through gradient boosting complements these capabilities, particularly advantageous for intricate classification tasks.

The hybrid approach of CNN, FractalNet and XGBoost can lead to better skin cancer detection and more accurate diagnosis. Existing diagnostic workflows can include this model as a supportive assistant to traditional diagnostic methods for dermatologists.

Potential Benefits:

Enhanced Prediction: The hybrid model provides more accurate predictions of skin lesions using methods from deep learning and boosting, assisting dermatologists in early detection of skin cancer.

Increased Efficiency: It minimizes the requirement for manual examination, accelerating the diagnostic workflow.

Received: July 25, 2025

Volume 38 No. 3s, 2025
ISSN: 1311-1728 (printed version); ISSN: 1314-8060 (on-line version)

Alternative Review: It can act as a supplementary opinion which could boost the diagnostic assurance in dubious situations.

Potential Challenges:

Integration Costs: AI tools need to be embedded into a practice and regular updates conducted which leads to financial outlay.

Practitioner Adoption Negative Effect: Dermatologists might find it difficult to adapt to AI models especially if they are not familiar with AI technologies.

Ethical considerations:

Data Privacy: AI systems process sensitive health data, which require strong privacy safeguards. Lack of adequate data privacy plans and location tracking risks could all put individuals at the risk of having their data compromised. Strict adherence to data protection regulations such as GDPR and HIPAA is critical to mitigate this.

Algorithmic Bias: AI algorithms could be trained on data with some biases, which can result in biased outcomes. The example of biased results in healthcare prediction What kind of data are you trained on? For example, An AI model trained on non-diverse datasets can not perform well for specific demographic groups, leading to the widening of the healthcare gap. Solution to this is curated data set and periodic audits of algorithms for fairness.

Misdiagnosis: AI systems could misdiagnose conditions because of data constraints or errors in the algorithm. AI can be a complementary tool but needs human oversight to validate diagnoses to prevent overreliance on technology.

Future research would outline potential directions for following areas to improve the accuracy of the model and its use:

Enhancing the model to analyze composite Biomedical Data: Further development may enable it to predict diseases more accurately as research shows that this composite modality improves prediction. Models that Synthesize Hypersensitive Data that combines Health Records, Imaging and Genetic analytics enhance robustness and accuracy.

Evaluating Clinical Feasibility of the Model to evaluate its exposure for use: We will plan to incorporate our further research by estimating the accuracy of the model in real patient environments with relation to existing therapies and possible clinical outcomes. The composite data could be all encompassing, consisting of family history, medications, treatments, age, occupation, language and ethnicity among others.

Potential Limitations

Study Design: It is true we may have faced some difficulties in generalizability as it depended on the sample. The sample size together with the demographic barrier was recorded, and we explained how these factors might affect the generalizability of the study results.

Received: July 25, 2025

Volume 38 No. 3s, 2025
ISSN: 1311-1728 (printed version); ISSN: 1314-8060 (on-line version)

Data: When stating the data limitations, we also cited possible biases that existed within the provided dataset such as diversity or completeness of data. We have outlined any possible gaps which may affect the comprehensive analysis as all attempts were to obtain excellent data.

Analysis: Indeed, we also considered that the selected methods and assumptions may have limited the scope of the analysis. Even though we used the established norm of the analytical process, we have also noted some methodological constraints such as possible overfitting and the limits of the tools used.

Conclusion

The HAM10000 skin cancer dataset was utilized to build a hybrid model that integrates XGBoost, Customized Convolutional Neural Networks (CNN), and FractalNet for the diagnosis and classification of skin cancer into seven types. In particular, this model capitalizes on the strengths of each component; XGBoost due to its strong predictive performance, CNNs for image processing and feature extraction, and the efficient use of parameters within the fractal architecture of FractalNet. Initially, data augmentation was performed to balance the dataset to ensure diversity in training data. The combined weak models were used with a meta decision model based on voting. The generalization for the integration of many of these models for different data is greater; thus, they are more adaptable to various situations. The hybrid model accuracy improved significantly to 98.69%. We expect this result to outpace that achieved with single models. In the future, more datasets and real images may help the classifier increase the robustness and applicability.

Abbreviation

Nil.

Acknowledgements

We would like to extend my heartfelt gratitude to Savitribai Phule Pune University for their unwavering support

throughout this research endeavor. Special acknowledgment is also due to my research guide, Dr. Sahebrao Bagal, for his invaluable support and guidance throughout this research. His expertise and encouragement have been helpful in the successful completion of this study.

Author Contributions

Mrs. S. R. Baji and Dr. S. B. Bagal contributed equally to the conceptualization, methodology, analysis, and writing of this article.

Conflict of Interest

The authors of this work state that they have no conflicts of interest about its publication.

Ethics Approval

Not Applicable.

Received: July 25, 2025

International Journal of Applied Mathematics

Volume 38 No. 3s, 2025

ISSN: 1311-1728 (printed version); ISSN: 1314-8060 (on-line version)

Funding

There was no internal/external funding for this research.

References

[1] Poon J, Wessel G M and Yajima M. An unregulated regulator: Vasa expression in the development of somatic cells and in tumorigenesis. Developmental Biology. 2016; 415(1):24-32. ”

[2] Kandoth C, McLellan M D, Vandin F, Ye K, Niu B, Lu C and Ding L. Mutational landscape and significance across 12 major cancer types. Nature. 2013; 502(7471):333-339. ”

[3] Egeberg A, Thyssen J P, Gislason G H and Skov L. Skin cancer in patients with psoriasis. Journal of the European Academy of Dermatology and Venereology. 2016; 30(8):1349-1353. ”

[4] Sabarwal A, Kumar K, Singh R P. Hazardous effects of chemical pesticides on human health–Cancer and other associated disorders. Environ. Toxicol. Pharmacol. 2018; 63:103–114. ”

[5] Franceschi S, Levi F, Randimbison L and La Vecchia C. Site distribution of different types of skin cancer: new aetiological clues. International journal of cancer. 1996; 67(1):24-28. ”

[6] Ciążyńska M, Kamińska-Winciorek G, Lange D, Lewandowski B, Reich A, Sławińska M and Lesiak A. The incidence and clinical analysis of non-melanoma skin cancer. Scientific reports. 2021; 11(1):4337. ”

[7] Dildar M, Akram S, Irfan M, Khan H U, Ramzan M, Mahmood A R and Mahnashi M H. Skin cancer detection: a review using deep learning techniques. International journal of environmental research and public health. 2010; 18(10):5479. ”

[8] Linares M A, Zakaria A and Nizran P, Skin cancer. Primary care: Clinics in office practice. 2015; 42(4):645-659. ”

[9] Freeman M and Laks S. Surveillance Imaging for Metastasis in High-Risk Melanoma: Importance in Individualized Patient Care and Survivorship. Melanoma Management. 2019; 6(1):MMT12. DOI: https://doi.org/10.2217/mmt-2019-0003. ”

[10] MacKie R M, Elwood J M and Hawk J L M. Links between exposure to ultraviolet radiation and skin cancer: a report of the Royal College of Physicians. Journal of the Royal College of Physicians of London. 1987; 21(2):91. ”

[11] Langholz B, Richardson J, Rappaport E, Waisman J, Cockburn M and Mack T. Skin characteristics and risk of superficial spreading and nodular melanoma (United States). Cancer Causes and Control. 2000; 11:741-750. ”

[12] Jackson A, Wilkinson C and Pill R. Moles and melanomas--who's at risk, who knows, and who cares? A strategy to inform those at high risk. British Journal of General Practice. 1999; 49(440):199-203. ”

[13] Hamidi R, Peng D and Cockburn M. Efficacy of skin self-examination for the early detection of melanoma. International journal of dermatology. 2010; 49(2):126-134. ”

Received: July 25, 2025

Volume 38 No. 3s, 2025

ISSN: 1311-1728 (printed version); ISSN: 1314-8060 (on-line version)

[14] Fernandes S L, Chakraborty B, Gurupur V P and Prabhu G A. Early skin cancer detection using computer aided diagnosis techniques. Journal of Integrated Design and Process Science. 2016; 20(1):33-43. ”

[15] Sharma D and Srivastava S. Automatically detection of skin cancer by classification of neural network, International Journal of Engineering and Technical Research. 2016; 4(1):15-18. ”

[16] Marchetti M A, Codella N C, Dusza S W, Gutman D A, Helba B, Kalloo A and International Skin Imaging Collaboration. Results of the 2016 International Skin Imaging Collaboration International Symposium on Biomedical Imaging challenge: Comparison of the accuracy of computer algorithms to dermatologists for the diagnosis of melanoma from dermoscopic images. Journal of the American Academy of Dermatology. 2018; 78(2):270-277. ”

[17] Hoffmann K, Gambichler T, Rick A, Kreutz M, Anschuetz M, Grünendick T and Altmeyer P. Diagnostic and neural analysis of skin cancer (DANAOS). A multicentre study for collection and computer-aided analysis of data from pigmented skin lesions using digital dermoscopy. British Journal of Dermatology. 2003; 149(4):801-809. ”

[18] Farooq M S, Arooj A, Alroobaea R, Baqasah A M, Jabarulla M Y, Singh D and Sardar R. Untangling computer-aided diagnostic system for screening diabetic retinopathy based on deep learning techniques. Sensors. 2022; 22(5):1803. ”

[19] Land W H and Verheggen E A. Experiments using an evolutionary programmed neural network with adaptive boosting for computer aided diagnosis of breast cancer. In Proceedings of the 2003 IEEE International Workshop on Soft Computing in Industrial Applications. SMCia/03. 2003;167-172. ”

[20] Narayanan D L, Saladi R N and Fox J L. Ultraviolet radiation and skin cancer. International journal of dermatology. 2010; 49(9):978-986. ”

[21] Celebi M E et al. A methodological approach to the clas- sification of dermoscopy images. Comput Med Imaging Graph. 2007; 31(6):362–373. ”

[22] Oliveira R B, Mercedes Filho E, Ma Z, Papa J P, Pereira A S, Tavares JMR. Computational methods for the image seg- mentation of pigmented skin lesions: a review. Comput Methods Progr Biomed. 2016; 131:127–141. ”

[23] Barata C, Celebi ME, Marques JS. Improving dermoscopy ımage classification using color constancy. IEEE J Biomed Health Informat. 2014; 19(3):1146–1152. ”

[24] Schaefer G, Rajab M, Celebi ME, Iyatomi H. Colour and contrast enhancement for improved skin lesion segmentation. Comput Med Imag Soc. 2010; 35:99–104. ”

[25] Iyatomi H, Celebi ME, Schaefer G, Tanaka M. Automated color calibration method for dermoscopy images. Comput Med Imag Soc. 2010; 35:89–98. ”

[26] Zhang J, Xie Y, Wu Q, Xia Y. Medical ımage classification using synergic deep learning. Med Imag Anal. 2019; 54:10–19. ”

[27] Fatima R, Khan MZA, Dhruve KP. Computer aided multi- parameter extraction system to aid early detection of skin cancer melanoma. Int J Comput Sci Netw Secur. 2012; 12(10):74–86. ”

Received: July 25, 2025

Volume 38 No. 3s, 2025

ISSN: 1311-1728 (printed version); ISSN: 1314-8060 (on-line version)

[28] Qian C et al. A detection and segmentation architecture for skin lesion segmentation on dermoscopy ımages.ArXiv, arXiv:1809.03917. 2018. ”

[29] Ercal F, Chawla A, Stoecker WV, Lee HC, Moss RH. Neural network diagnosis of malignant melanoma from color images. IEEE Trans Biomed Eng. 1994; 41(9):837–845. ”

[30] Ercal F et al. Skin Cancer Diagnosis using Hierarchical Neural Networks and Fuzzy Systems. Artificial Neural Networks in Engineering - Proceedings (ANNIE'94). 1994; (4):613-618. ”

[31] Binder M, Steiner A, Schwarz M, Knollmayer S, Wolff K, Pehamberger H. Application of an artificial neural network in epiluminescence microscopy pattern analysis of pigmented skin lesions: a pilot study. Br J Dermatol. 1994; 130(4):460–465. ”

[32] Pereira PMM et al. Skin lesion classification enhancement using border-line features—the melanoma vs nevus problem. Biomed Signal Process Control. 2020; 57:101765. ”

[33] Almaraz-Damian J-A, Ponomaryov V, Sadovnychiy S, Castille- jos-Fernandez H. Melanoma and nevus skin lesion clas- sification using handcraft and deep learning feature fusion via mutual information measures. Entropy. 2020; 22(4):484. ”

[34] Kavitha J C and Suruliandi A. Texture and color feature extraction for classification of melanoma using SVM. 2016 International Conference on Computing Technologies and Intelligent Data Engineering (ICCTIDE'16). Kovilpatti. India. 2016; 1-6. DOI: 10.1109/ICCTIDE.2016.7725347. ”

[35] Hu Z, Tang J, Wang Z, Zhang K, Zhang L, Sun Q. Deep learning for image-based cancer detection and diagnosis–a sur- vey. Pattern Recogn. 2018; 83:134–149. ”

[36] Mahbod A, Schaefer G, Ellinger I, Ecker R, Pitiot A, Wang C. Fusing fine-tuned deep features for skin lesion classifi- cation. Comput Med Imaging Graph. 2019; 71:19–29. ”

[37] Kawahara J, BenTaieb A, Hamarneh G. Deep features to classify skin lesions. In: 2016 IEEE 13th International sympo- sium on biomedical imaging (ISBI). 2016; 1397-1400. ”

[38] Zhang J, Xie Y, Xia Y, Shen C. Attention residual learning for skin lesion classification. IEEE Trans Med Imag. 2019; 38(9):2092–2103. ”

[39] Bi L, Feng DD, Fulham M, Kim J. Multi-Label classification of multi-modality skin lesion via hyper-connected con-volutional neural network. Pattern Recogn. 2020; 107:107502. ”

[40] Ayan E, Unver HM. Data augmentation importance for classification of skin lesions via deep learning. In: 2018 Electric electronics, computer science, biomedical engineerings’ meeting (EBBT). 2018; 1–4. DOI: 10.1109/EBBT.2018.8391469. ”

[41] Menegola A, Fornaciali M, Pires R, Bittencourt FV, Avila S, Valle E. Knowledge transfer for melanoma screening with deep learning. In: 2017 IEEE 14th International symposium on biomedical imaging (ISBI 2017). 2017; 297–300. ”

[42] Lopez A R, Giro-i-Nieto X, Burdick J, Marques O. Skin lesion classification from dermoscopic images using deep learn- ing techniques. In:2017 13th IASTED International conference on biomedical engineering (BioMed). 2017; 49–54. ”

Received: July 25, 2025

Volume 38 No. 3s, 2025

ISSN: 1311-1728 (printed version); ISSN: 1314-8060 (on-line version)

[43] Mahbod A, Schaefer G, Wang C, Dorffner G, Ecker R, Ellinger I. Transfer learning using a multi-scale and multi-network ensemble for skin lesion classification. Comput Methods Programs Biomed. 2020; 193:105475. ”

[44] Gessert N, Nielsen M, Shaikh M, Werner R, Schlaefer A. Skin lesion classification using ensembles of multi-resolution EfficientNets with meta data. MethodsX. 2020; 7:100864. DOI:https://doi.org/10.1016/j.mex.2020.100864. ”

[45] Yilmaz E, Trocan M. Benign and malignant skin lesion classification comparison for three deep-learning architectures. In: Asian conference on intelligent information and database systems. 2020; (12033):514–524. DOI:https://doi.org/10.1007/978-3-030-41964-6_44. ”

[46] Salian A C, Vaze S, Singh P, Shaikh G N, Chapaneri S, Jayaswal D. Skin lesion classification using deep learning archi- tectures. In: 2020 3rd International conference on communication system, computing and IT applications (CSCITA), 2020; 168–173. DOI:10.1109/CSCITA47329.2020.9137810. ”

[47] Serte S and Demirel H. Gabor wavelet-based deep learning for skin lesion classification. Comput Biol Med. 2019; 113:103423. ”

[48] Liu L, Mou L, Zhu XX, Mandal M. Automatic skin lesion classification based on mid-level feature learning. Comput Med Imag Graph. 2020; 84:101765. ”

[49] Milton MAA. Automated skin lesion classification using ensemble of deep neural networks in ISIC 2018: Skin lesion analysis towards melanoma detection challenge. 2019. DOI:https://doi.org/10.48550/arXiv.1901.10802. ”

[50] Alzubaidi L, Zhang J, Humaidi A J, Al-Dujaili A, Duan Y, Al-Shamma O and Farhan L. Review of deep learning: Concepts, CNN architectures, challenges, applications, future directions. Journal of big Data. 2021; (8)1-74. ”

[51] Zhang M, Li W and Du Q. Diverse region-based CNN for hyperspectral image classification. IEEE Transactions on Image Processing. 2018; 27(6):2623-2634. ”

[52] Larsson G, Maire M and Shakhnarovich G. Fractalnet: Ultra-deep neural networks without residuals. 2017; (4). DOI:https://doi.org/10.48550/arXiv.1605.07648. ”

[53] Yang W, Wang S, Xu D, Wang X and Liu J. Towards scale-free rain streak removal via self-supervised fractal band learning. In Proceedings of the AAAI Conference on Artificial Intelligence. 2020; 34(7):12629-12636. ”

[54] Chakraborty B, Sawada Y and Chakraborty G. Layered fractal neural net: computational performance as a classifier. Knowledge-Based Systems. 1997; 10(3):177-182. ”

[55] Chen T and Guestrin C. Xgboost: A scalable tree boosting system. In Proceedings of the 22nd ACM SIGKDD international conference on knowledge discovery and data mining. 2016; 785-794. DOI:https://doi.org/10.1145/2939672.2939785. ”

[56] Chakraborty S and Bhattacharya S. Application of XGBoost algorithm as a predictive tool in a CNC turning process. Reports in Mechanical Engineering. 2021; 2(1):190-201. ”

Received: July 25, 2025

Volume 38 No. 3s, 2025

ISSN: 1311-1728 (printed version); ISSN: 1314-8060 (on-line version)

[57] Ma M, Zhao G, He B, Li Q, Dong H, Wang S and Wang Z. XGBoost-based method for flash flood risk assessment. Journal of Hydrology. 2021; 598:126382. ”

[58] Zhu W, Zeng N and Wang N. Sensitivity, specificity, accuracy, associated confidence interval and ROC analysis with practical SAS implementations. NESUG Proceedings: Health Care and Life Sciences. Baltimore, Maryland. 2010; (19):67.”

[59] Goutte C and Gaussier E. A probabilistic interpretation of precision, recall and F-score, with implication for evaluation. In European Conference on Information Retrieval. Springer, Berlin, Heidelberg. 2005;(3408):345-359. DOI:https://doi.org/10.1007/978-3-540-31865-1_25. ”

[60] Davis J and Goadrich M. The relationship between Precision-Recall and ROC curves. In Proceedings of the 23rd International Conference on Machine Learning. 2006; 233-240. DOI:https://doi.org/10.1145/1143844.1143874. ”

[61] Juba B. and Le H. S. Precision-recall versus accuracy and the role of large data sets. In Proceedings of the AAAI Conference on Artificial Intelligence. 2019; 33(01):4039-4048. ”

[62] Deng X, Liu Q, Deng Y and Mahadevan S. An improved method to construct basic probability assignment based on the confusion matrix for classification problem. Information Sciences. 2016; 340:250-261. ”

[63] Noel Codella, Veronica Rotemberg, Philipp Tschandl, M Emre Celebi, Stephen Dusza, David Gutman, Brian Helba, Aadi Kalloo, Konstantinos Liopyris, Michael Marchetti, Harald Kittler, Allan Halpern. Skin Lesion Analysis Toward Melanoma Detection 2018: A Challenge Hosted by the International Skin Imaging Collaboration (ISIC). 2018;(2). DOI:https://doi.org/10.48550/arXiv.1902.03368. ”

[64] Tschandl P, Rosendahl C and Kittler H. The HAM10000 dataset, a large collection of multi-source dermatoscopic images of common pigmented skin lesions. Sci. Data. 2018; (5):180161. ”

[65] Harangi B. Skin lesion classification with ensembles of deep convolutional neural networks. J. Biomed. Inform. 2018; (86):25–32. ”

[66] Codella N C, Nguyen Q B, Pankanti S, Gutman D A, Helba B, Halpern A C and Smith J R. Deep learning ensembles for melanoma recognition in dermoscopy images. IBM J. Res. Develop. 2017; (61)4-5:1-5. ”

[67] Aboulmira A , Raouhi E M, Hrimech H and Lachgar M. Ensemble learning methods for deep learning: Application to skin lesions classification. Proc. 11th Int. Symp. Signal, Image, Video Commun. (ISIVC). 2022; 1–6. ”

[68] Alizadeh S M and Mahloojifar A. Automatic skin cancer detection in dermoscopy images by combining convolutional neural networks and texture features. Int. J. Imag. Syst. Technol. 2021; (31)2:695–707. ”

[69] Pacheco AGC and Krohling R A. An attention-based mechanism to combine images and metadata in deep learning models applied to skin cancer classification. IEEE J. Biomed. Health Informat. 2021; (25)9:3554–3563. ”

Received: July 25, 2025

Volume 38 No. 3s, 2025

ISSN: 1311-1728 (printed version); ISSN: 1314-8060 (on-line version)

[70] Toğaçar M, Cömert Z and Ergen B. Intelligent skin cancer detection applying autoencoder, MobileNetV2 and spiking neural networks. Chaos, Solitons Fractals. 2021; (144):110714. ”

[71] Nawaz M, Mehmood Z, Nazir T, Naqvi R A, Rehman A, Iqbal M and Saba T. Skin cancer detection from dermoscopic images using deep learning and fuzzy k-means clustering. Microsc. Res. Technique. 2022; 85(1):339–351. ”

[72] Ali M S, Miah M S, Haque J, Rahman M M and Islam M K. An enhanced technique of skin cancer classification using deep convolutional neural network with transfer learning models. Mach. Learn. Appl.Se. 2021; (5) Art. no. 100036. ”

[73] Imran A, Nasir A, Bilal M, Sun G, Alzahrani A and Almuhaimeed A. Skin cancer detection using combined decision of deep learners. IEEE Access. 2022; (10)118198-118212. ”

S. Baji (Seema Baji) received B. E. degree in E&TC from Jawaharlal Nehru College Engineering, Sambhaji Nagar (Aurangabad) affiliated to Dr. B. A. M. U., Sambhaji Nagar (Aurangabad), Maharashtra in 2007. M. Tech Degree in Electronics from Jawaharlal Nehru College Engineering, Sambhaji Nagar (Aurangabad) affiliated to Dr. B. A. M. U., Sambhaji Nagar (Aurangabad), Maharashtra in 2010. She is currently working toward the Ph.D. degree at the Department of Electronics and Telecommunication Engineering, Sanjivani College of Engineering, Kopargaon, Maharashtra, India. Her research interests include Deep learning and machine learning application in Image processing.

S. Bagal (Sahebrao Bagal) received B. E. degree in Electronics from K. K. Wagh Institute of Engineering Education and Research, Nashik affiliated to Savitribai Phule University of Pune, Pune, Maharashtra in 1993. M. E. Degree in Electronics from S. R. T. M. University, Nanded, Maharashtra in 2002. Ph.D. degree in E&TC from S. R. T. M. University, Nanded, Maharashtra, India in 2016. His research interests include image processing and soft computing.

Received: July 25, 2025

International Journal of Applied Mathematics
Volume 38 No. 3s, 2025
ISSN: 1311-1728 (printed version); ISSN: 1314-8060 (on-line version)

S. Chaudhari (Sachin Chaudhari) received B. E. degree in Electronics from North Maharashtra University, Jalgaon, Maharashtra in 2004. M. E. Degree in Electronics from Sinhghad COE, Vadgaon, Pune - SPPU Pune, Maharashtra in 2014. Ph.D. degree in Electronics from Shri Jagdish Jhabarmal University – Vidyanagar, Rajasthan, India in 2018. His research interests include image processing, Digital Communication and Digital Signal Processing.

B. Agarkar (Balasaheb Agarkar) received B. E. degree in Electronics from Dr. B. A. M. U., Sambhaji Nagar (Aurangabad) in 1990. M. E. Degree in Electronics from Dr. B. A. M. U., Sambhaji Nagar (Aurangabad) in 1999. Ph.D. degree in E&TC from S. R. T. M. University, Nanded, Maharashtra, India in 2016. His research interests include Neural Network, machine learning and Computer Networks.

Received: July 25, 2025